Influence of Electron and Ion Pressure Near the Lower Hybrid Resonance

R. BABU, B. LAMMERS, and H. SCHLÜTER

Ruhr University, Bochum

(Z. Naturforsch. **27 a**, 930—938 [1972]; received 28 January 1972)

Near the lower hybrid resonance the power transfer from electromagnetic waves to a plasma cylinder is calculated with the inclusion of electron and ion pressures. Ion-electron collisions are accounted for in addition to the collisions of charged particles with neutrals. Drastic deviations from calculations neglecting the pressure effects occur for plasmas of low electron density and/or small radial extent. Different ranges of a specific ratio comparing the influence of collision with that of pressure terms are investigated.

I. Introduction

In a previous analysis [1] of radio frequency power transfer – from an azimuthally symmetric excitation coil to a magnetized homogeneous plasma cylinder – the electron pressure has been incorporated and its influence in the range of the lower hybrid resonance has been found to be small for conditions of recent experimental interest [2]. This finding, the cold plasma treatment to be a good approximation, cannot be expected in general as pointed out previously [1, 3]. The main object of this investigation is therefore to survey other conditions, to present and discuss situations for which inclusion of pressure effects causes important – even drastic – changes indeed.

The following discussions and numerical calculations are based on a fluid treatment and resultant general expressions for plasma impedances and power transfer similar to those obtained in the preceding analysis. However, non-zero ion pressure is also included. Moreover ion-electron collisions are taken into account in addition to collisions with neutral particles.

II. Power Transfer Relations

Momentum transfer equations as used in I [relations (1)] including collision terms as well as terms due to electron and ion pressure, are taken as basis and linearized with respect to perturbations with time dependencies $\sim\exp\{-i\,\omega\,t\}$. In the following the approximate form of collision terms – sufficient for the situations envisaged in I – is replaced by the exact and complete expressions as given and discussed in the basic study of SCHLÜTER [4]. Allowing for increasing degrees of ionization, the ion-neutral collision term $\nu_i \boldsymbol{v}_i$ is rewritten to $\nu_{in}(\varrho_n/\varrho_i+\varrho_n)(\boldsymbol{v}_i-\boldsymbol{v}_n)$, the electron-neutral collision term $\nu_e \boldsymbol{v}_e$ to $\nu_{en}(\varrho_n/\varrho_e+\varrho_n)(\boldsymbol{v}_e-\boldsymbol{v}_n)$. Consistently ion-electron collisions are included by a term $-\nu_{ie}(\varrho_e/\varrho_i+\varrho_e)(\boldsymbol{v}_i-\boldsymbol{v}_e)$ on the right hand side of the ion momentum equation and a corresponding term in the electron momentum equation. ϱ_i, ϱ_e, and ϱ_n are the particle mass densities. It should be noted that the common approach to the collisions with neutrals (as used in I) neglects perturbations of the neutral fluid, in particular the co-motion of the neutrals expressed by $\boldsymbol{v}_n$. However, the expectations of this to be a good approximation in practically all situations of interest, has been checked numerically by inspection of the exact dispersion relation (with $T_e \neq 0$, $T_i = 0$) and of resultant correction terms in the ensuing impedance relations; therefore the co-motion of the neutrals is again neglected in the following.

Combination of the momentum equations with the continuity and Maxwellian equations leads to a dispersion relation of third order in the propagation constant squared, $k_\perp{}^2$, as already given by (5) in I with $\nabla_\perp$ replaced by $i\boldsymbol{k}_\perp$. In order to avoid unnecessary algebraic complexities, the assumption $(\nu_{ie}/\omega)^2 \ll 1$ is made which is always well fulfilled in the following. Due to the inclusion of ion-electron collisions the quantities ω_j, β_j, and A_j (j = e, i) occuring in (5) of I are modified, as given by (A 1) to (A 6) of the Appendix.

The field quantities are now obtained in a manner analogous to that in I. The amplitude of the radio frequency magnetic field strength in the

Reprint requests to Prof. Dr. H. SCHLÜTER, Lehrstuhl II – Institut für Experimentalphysik, Ruhr-Universität Bochum, D-4630 *Bochum-Querenburg*, Postfach 2148.

plasma, $H_z^{(p)}$, has three terms:

$$H_z^{(p)} = [A_n J_n(k_1 r) + B_n J_n(k_2 r) + B_n' J_n(k_3 r)]\, e^{in\Theta}. \tag{1}$$

k_1^2, k_2^2, k_3^2 are the three roots for the third order dispersion relation for $k_\perp^2$ with $T_i \neq 0$. The additional boundary condition required is taken to be (at the plasma radius $r = p$)

$$(\hat{e}_r \cdot \boldsymbol{v}_i) = 0, \tag{2}$$

as usually employed (see for example Ref. [3]).

Proceeding similarly as in I the impedance for a plasma of radius p surrounded by a coil of radius s is obtained. The inclusion of ion temperature terms results in the following extension of (39) in I, the structure and meaning of which has been discussed earlier:

$$\frac{Z_t}{R_c} = \pm \frac{\{I_2 I_{\Theta 1} - I_1 k_0 p J_n(k_1 p)\} + (B_n/A_n)\{I_2 I_{\Theta 2} - I_1 k_0 p J_n(k_2 p)\} + (B_n'/A_n)\{I_2 I_{\Theta 3} - I_1 k_0 p J_n(k_3 p)\}}{\left\{\frac{H_n(k_0 p)}{H_n'(k_0 s)} I_{\Theta 1} - \frac{k_0 p H_n'(k_0 p)}{H_n'(k_0 s)} J_n(k_1 p)\right\} + \frac{B_n}{A_n}\left\{\frac{H_n(k_0 p)}{H_n'(k_0 s)} I_{\Theta 2} - \frac{k_0 p H_n'(k_0 p)}{H_n'(k_0 s)} J_n(k_2 p)\right\} + \frac{B_n'}{A_n}\left\{\frac{H_n(k_0 p)}{H_n'(k_0 s)} I_{\Theta 3} - \frac{k_0 p H_n'(k_0 p)}{H_n'(k_0 s)} J_n(k_3 p)\right\}}. \tag{3}$$

The various quantities involved above are explicitely defined by (A 7) to (A 21) of the Appendix.

The power transfer is given in the case of known coil current I_Θ by

$$L_t = \tfrac{1}{2} |I_\Theta|^2 R_e(Z_t) \tag{4}$$

and in the case of known coil voltage U by

$$L_t = \tfrac{1}{2} |U|^2 R_e(Z_t)/|Z_t|^2. \tag{5}$$

L_t represents the power dissipated in the plasma and radiated to infinity. The latter fraction is usually unimportant; if required it may also formally be excluded by rearrangement of the derivation along the lines indicated in I.

III. Modifications due to Pressure Effects

In order to discuss the domain of strong – and complementarily of weak – pressure influence initially the ion pressure shall be neglected ($p_i = 0$). This allows a direct connection to the findings of I and a more systematic procedure. The modifications due to finite p_i shall be considered subsequently.

1. Weak Pressure Influence

The power transfer in the range of the lower hybrid resonance resulting from the above warm plasma treatment – accounting for finite p_e – is virtually identical to that resulting from the cold plasma treatment neglecting p_e, provided the relation

$$k_{cr} \cdot p \gtrsim \pi \tag{6}$$

characterizing the occurrence of radial eigenmodes [5], and the relation

$$\nu^2/\omega^2 \gg 2\gamma_e k T_e N_e/(B_0^2/2\mu_0), \tag{7}$$

signifying the predominance of collision terms over pressure terms [6, 7], are fulfilled. These two conditions and their consequences are discussed in more details in the following. They can be ascertained by inspection of the leading terms of (3) and by numerical comparisons. k_{cr} is the (positive) real part of the plasma propagation constant k_c as resulting from the cold plasma treatment with $p_e = 0$. Its value close to the lower hybrid frequency

$$\omega_{LH} = \left\{\Omega_i \Omega_e \frac{\omega_{pe}^2 + \Omega_i \Omega_e}{\omega_{pe}^2 + \Omega_e^2}\right\}^{1/2}$$

is given in good approximation by

$$\omega_{pe}/c \cdot \sqrt{\omega/2\nu}.$$

The collision frequency relevant in this context is given by

$$\nu = \nu_{en} \frac{\varrho_n}{\varrho_e + \varrho_n} + \nu_{ie} + \nu_{in} \frac{\varrho_n}{\varrho_i + \varrho_n} \frac{\Omega_i \Omega_e}{\omega^2}, \tag{8}$$

neglecting ϱ_e compared to ϱ_i and ν_{in}^2 compared to ω^2. Analysis of the dispersion relation shows that the collision frequencies occur in the above grouping at the decisive places [5, 7].

As will be demonstrated, relation (6) is generally more important than relation (7). The former relation ensures the appearance of geometrical coupling resonances connected with radial modes as predicted by the cold plasma treatment. The occurrence of these modes and the resulting maxima of power transfer is the significant and dominant feature of plasma behavior in the range of the lower hybrid frequency (within the frame work of theoretical treatment considered here); these power maxima occur in the vicinity of the lower hybrid frequency with $\omega \lesssim \omega_{LH}$.

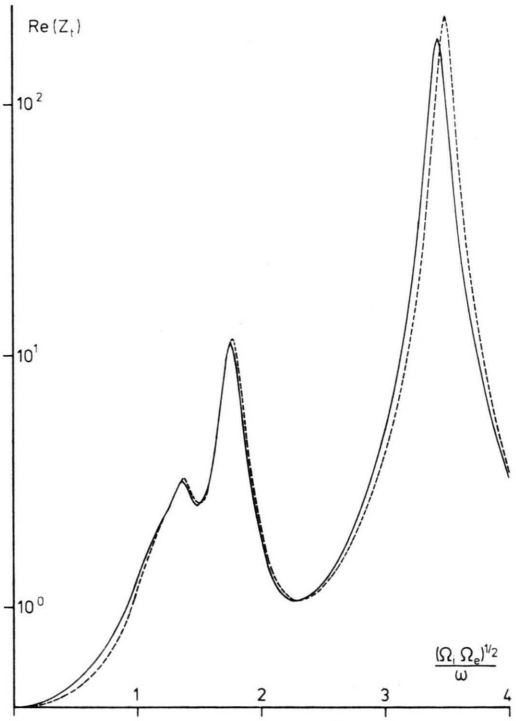

Fig. 1. Normalized power transfer ($L_t/|I_\Theta/2|^2$) with constant coil current. The parameters are: $\omega/2\pi=29.6$ MHz, $s=p=3.0$ cm, $N_n=5\cdot10^{14}$ cm^{-3}, $N_e=2\cdot10^{12}$ cm^{-3}, $T_e=10^5$ °K, $T_i=0$, $\nu_{en}=5\cdot10^7$ s^{-1}, $\nu_{in}=2.5\cdot10^6$ s^{-1}, $\nu_{ie}=2.08\cdot10^6$ s^{-1}.

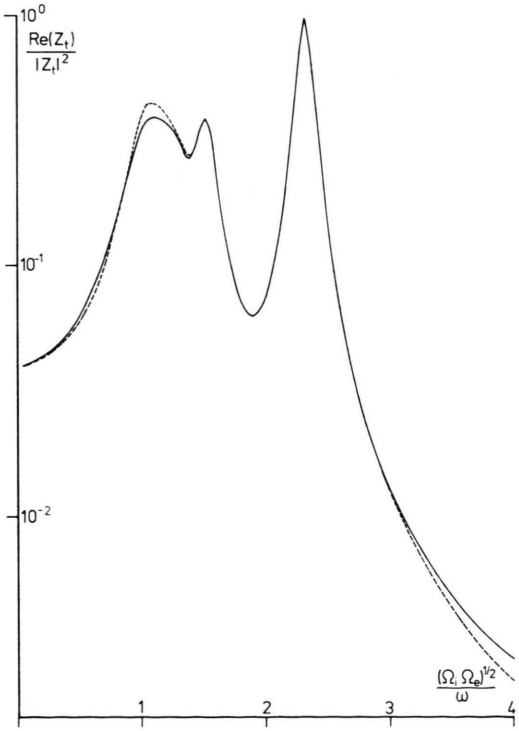

Fig. 2. Normalized power transfer ($L_t^2/|U/2|^2$) at a constant coil voltage. All data as in Figure 1.

Situations fulfilling conditions (6) and (7) – with $p_e \neq 0$, $p_i = 0$ – are illustrated by Figures 1 and 2. Dotted curves always represent comparative calculations of the cold plasma approach ($p_e = p_i = 0$). In all figures the abscissa always represents $(\Omega_i \Omega_e)^{1/2}/\omega$, and the coil width is 5 cm. Singly ionized hydrogen plasma is considered in consistence with the experimental objectives. In the case of constant current I_Θ of the excitation coil (Fig. 1) the minima of $J_0(k_c p)$ are responsible for the power maxima ("free oscillations"), whereas for the case of the coil voltage U being considered to be constant (Fig. 2), the minima of $J_1(k_c p)$ are related to the power maxima ("forced oscillations"). The latter behavior is due to the drastic changes of $U/I_\Theta = Z$ with $k_c p$. It transforms towards the behavior of constant I_Θ, when the gap between excitation coil and plasma column $s-p$ grows from zero to a sizeable fraction of p (Fig. 3).

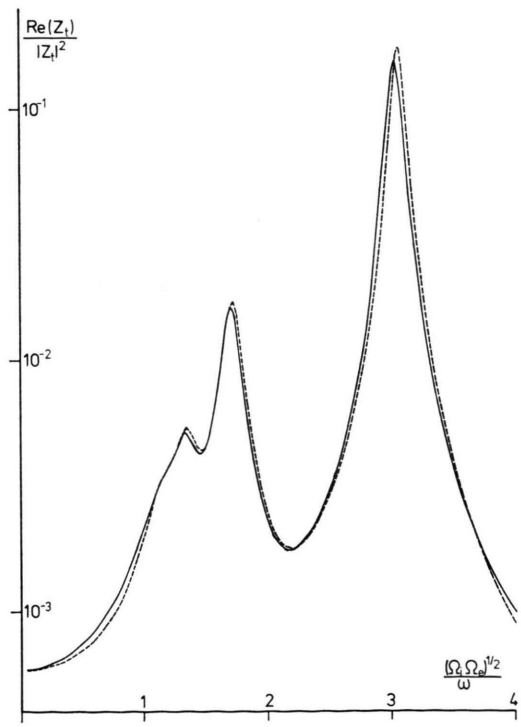

Fig. 3. Normalized power transfer ($L_t^2/|U/2|^2$) at a constant coil voltage including a finite coil-plasma gap: $s=5.0$ cm, $p=3.0$ cm. All data as in Figure 1.

Relation (7) is a necessary and sufficient condition so that one of the roots of $k_\perp^2$ is virtually identical with k_c^2 (single solution for $p_e = 0$) not only for $\omega < \omega_{LH}$ and $\omega > \omega_{LH}$, but even in the im-

mediate vicinity of the lower hybrid frequency, i. e. for $\omega \approx \omega_{LH}$. As far as the power transfer is concerned, violations of relation (7) have no appreciable effect, as demonstrated by Fig. 4 (violation by

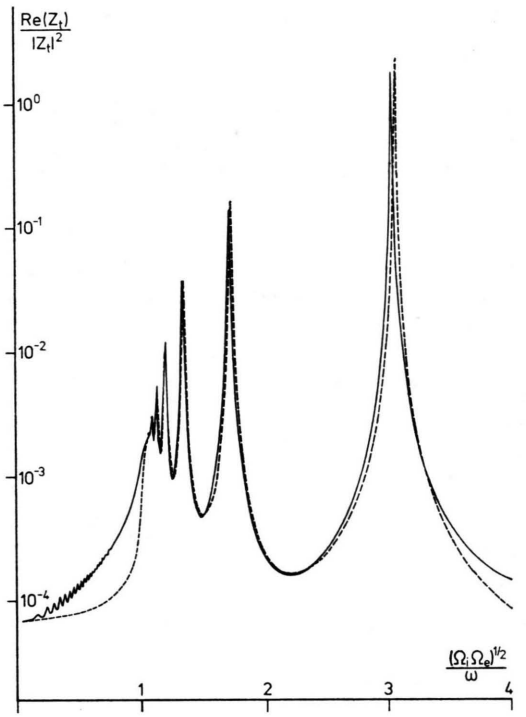

Fig. 4. Normalized power transfer when condition (28) is violated. $\omega/2\pi = 29.6$ MHz, $s = 5.0$ cm, $p = 3.0$ cm, $N_n = 2.5 \cdot 10^{13}$ cm^{-3}, $N_e = 2 \cdot 10^{12}$ cm^{-3}, $T_e = 10^5$ °K, $T_i = 0$, $\nu_{en} = 2.5 \cdot 10^6$ s^{-1}, $\nu_{in} = 1.25 \cdot 10^5$ s^{-1}, $\nu_{ie} = 2.08 \cdot 10^6$ s^{-1}.

a factor of ~ 10); only the wing $\omega > \omega_{LH}$ is noticeably influenced. More pronounced changes and deviations from the cold plasma treatment in the domain $\omega \gtrsim \omega_{LH}$ appear when condition (7) is drastically violated; in Fig. 5 an example is shown with relation (7) being violated by a factor 200; larger factors lead, of course, to even more extensive changes. The various power peaks occuring in Figs. 4 and 5 are the geometrical coupling resonances and are related to the radial eigenmodes; the peaks for $\omega \lesssim \omega_{LH}$ are the well known coupling resonances of the cold plasma approximation.

Additional structures may appear in the range $\omega > \omega_{LH}$, which can be traced to geometrical coupling resonances of radial modes connected with the additional solution of $k_\perp^2$ obtained by the assumption of finite p_e. The wing $\omega < \omega_{LH}$ is affected to a – comparatively – limited extent. The geometric

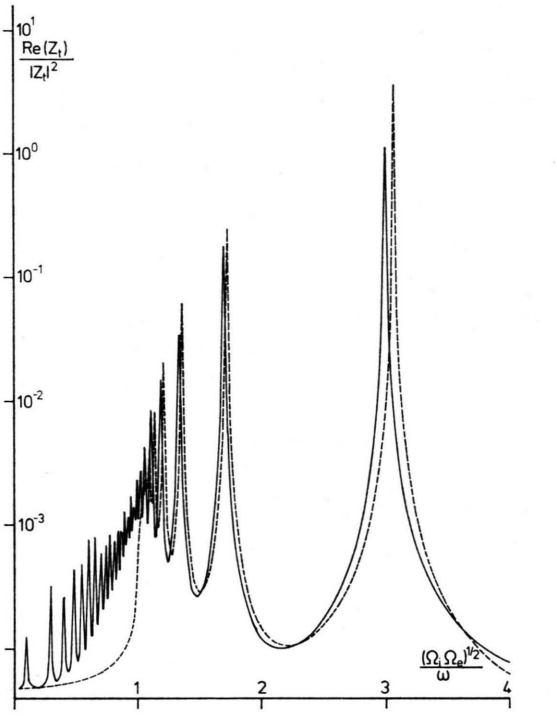

Fig. 5. Normalized power transfer with drastic violations of condition (28). All data as in Fig. 4 except $T_e = 6 \cdot 10^5$ °K and correspondingly $\nu_{ie} = 1.72 \cdot 10^5$ s^{-1}.

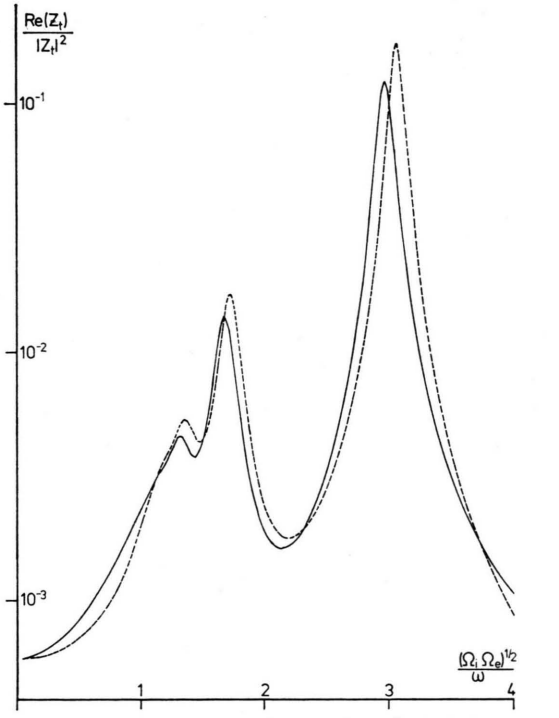

Fig. 6. Normalized power transfer at relatively high ion temperature $T_i = 10\, T_e = 10^6$ °K. Finite gap: $s = 5.0$ and $p = 3.0$ is included and the other data are same as in Figure 1.

coupling resonances resulting from the cold plasma treatment are not completely erased and remain to be the dominant features in the range of the lower hybrid frequency even under these conditions.

So far the ion pressure has been set zero in this chapter. As long as conditions (6) and (7) are fulfilled and thus the inclusion of finite p_e is not important in this context, the inclusion of finite p_i does not cause drastic changes either; even relatively high ion temperatures do not cause major changes, as illustrated by Fig. 6 for $T_i = 10\,T_e$ (conditions related to those of Figure 3). The structure in the left wing of the lower hybrid resonance ($\omega > \omega_{LH}$) pointed out in context of Figs. 4 and 5 is influenced by inclusion of finite T_i; the number of smal peaks in this domain is generally decreasing with increasing T_i.

2. *Strong Pressure Influence*

As soon as relation (6) is violated, strong changes due to finite p_e may occur, the cold plasma treatment becoming a poor approximation. The domineering feature of coupling resonances in the domain $\omega \lesssim \omega_{LH}$ due to radial modes linked to that root of $k_\perp{}^2$ which closely resembles the cold plasma solution $k_c{}^2$, cannot be realized. The previously secondary role of radial modes for $\omega > \omega_{LH}$ (linked to the other "warm" root of $k_\perp{}^2$, which is introduced by finite p_e) may now become prominent and decisively determines the structuring of transfered power as a function of the static magnetic field strength (or of the wave frequency). For Fig. 7 relation (6) is violated, though relation (7) is yet fulfilled. The curve for $p_e \neq 0$ differs considerably from that for $p_e = 0$; the peak of the solid curve is related to a radial mode introduced by finite p_e as discused above. A situation with relation (6) as well as relation (7) being violated is considered in Figure 8. Two radial modes for $\omega > \omega_{LH}$ are prominent, and again there are considerable deviations from the cold plasma treatment. As pointed out before, in a narrow range around $\omega = \omega_{LH}$ none of the two roots of $k_\perp{}^2$ for $p_e \neq 0$ is reminiscent of the single root for $p_e = 0$, when the relation (7) is violated.

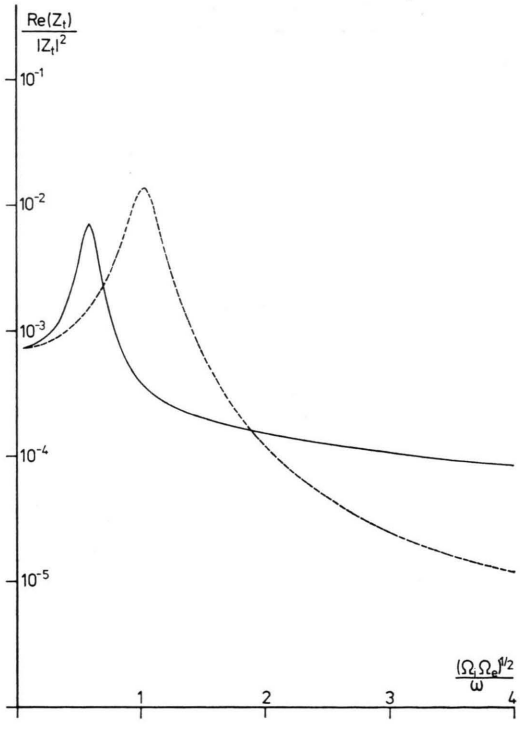

Fig. 7. Normalized power transfer for a relatively thin plasma of small radial extent with condition (28) being fulfilled. $s = 0.5$ cm, $p = 0.3$ cm, $\omega/2\pi = 7$ MHz, $N_n = 2.7 \cdot 10^{14}$ cm^{-3}, $N_e = 2 \cdot 10^{10}$ cm^{-3}, $T_e = 10^5$ °K, $T_i = 2 \cdot 10^3$ °K, $\nu_{en} = 10^7$ s^{-1}, $\nu_{in} = 5 \cdot 10^5$ s^{-1}, $\nu_{ie} = 2.46 \cdot 10^4$ s^{-1}.

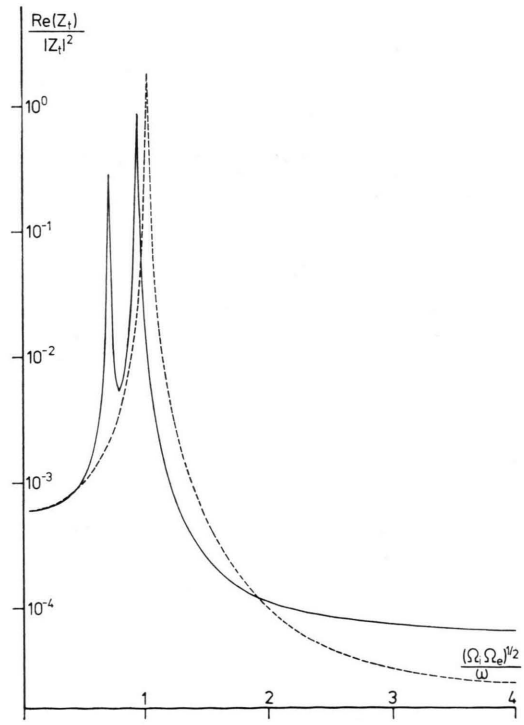

Fig. 8. Normalized power transfer for a thin plasma with condition (28) violated. $s = 0.5$ cm, $p = 0.3$ cm, $\omega/2\pi = 29.6$ MHz, $N_n = 3.2 \cdot 10^{13}$ cm^{-3}, $N_e = 9 \cdot 10^{11}$ cm^{-3}, $T_e = 4 \cdot 10^5$ °K, $T_i = 0$, $\nu_{en} = 3.2 \cdot 10^6$ s^{-1}, $\nu_{in} = 3.7 \cdot 10^4$ s^{-1}, $\nu_{ie} = 1.4 \cdot 10^5$ s^{-1}.

In situations with strong influence of the electron pressure, such as depicted in Figs. 7 and 8, also the influence of the ion pressure may be expected to be stronger than in the preceding section, in particular when p_i becomes comparable with p_e. This is fully born out by the typical examples given in Figures 9 and 10. Except for the non-zero ion temperature

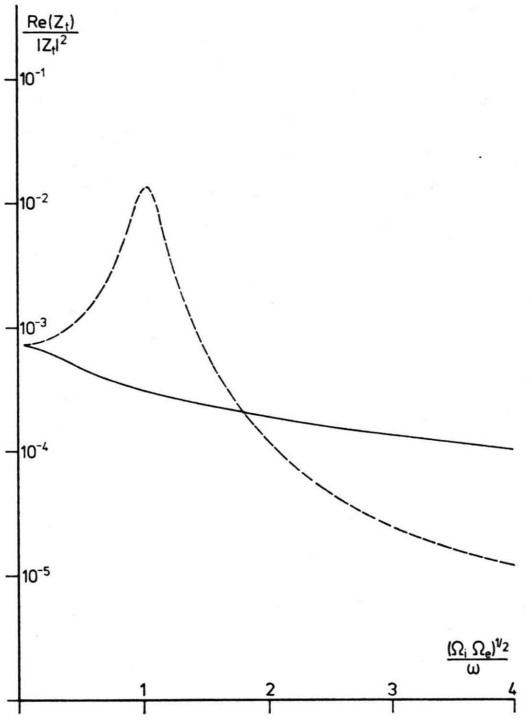

Fig. 9. Normalized power transfer with high ion temperature $T_i = T_e$ for parameters of Figure 7.

($T_i = T_e$), Fig. 9 envisages the same conditions as that of Fig. 7. The peak of the solid curve to be seen before has been virtually erased by the presence of finite p_i ($= p_e$). In Fig. 10 – to be related to Fig. 8 – the solid curve has retained only one peak.

IV. Influence of Various Collision Terms

So far examples with relatively strong electron neutral collision frequencies ν_{en} have been considered facilitating comparisons to I. By (8) an effective collision frequency – weighting the contributions of the three collisions considered – is defined in a certain context; it reflects the comparative influence of these collision frequencies in one

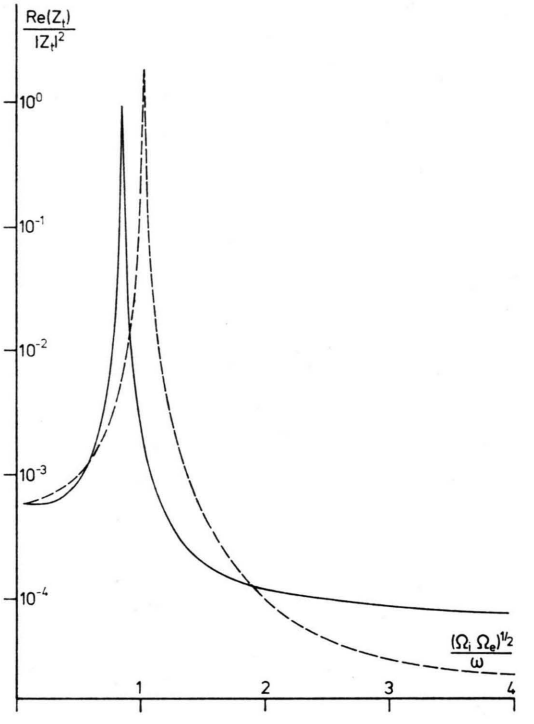

Fig. 10. Normalized power transfer with high ion temperature $T_i = T_e$ for parameters of Figure 8.

coefficient of the dispersion relation and does not account for different grouping in other coefficients and should thus not necessarily be representative for the influence of the various collision frequencies in the final power expressions. Nevertheless it may be hoped that the weighting in (8) gives an approximation at least in the case of weak pressure influence. This expectation can be substantiated by comparative calculations with only one of the three ν_{ie}, ν_{en}, and ν_{in} being the non-zero collision frequency with the same value in each case. [The density factors in (8) are practically unity for the cases plotted.] In Fig. 11 a typical situation of weak pressure influence is studied: Indeed ν_{ie} and ν_{en} have – practically – the same influence on the power curves, whereas ν_{in} appears to have larger influence for $\Omega_i \Omega_e > \omega^2$ and weaker influence for $\Omega_i \Omega_e < \omega^2$, as suggested by the corresponding weight factor in (8). Comparative calculations for $p_e = p_i = 0$ are not included in the graphs any more.

When the pressure terms become important for the power calculations, the analysis of the influence of the three collision frequencies may seem to become more complicated. However, the behavior as

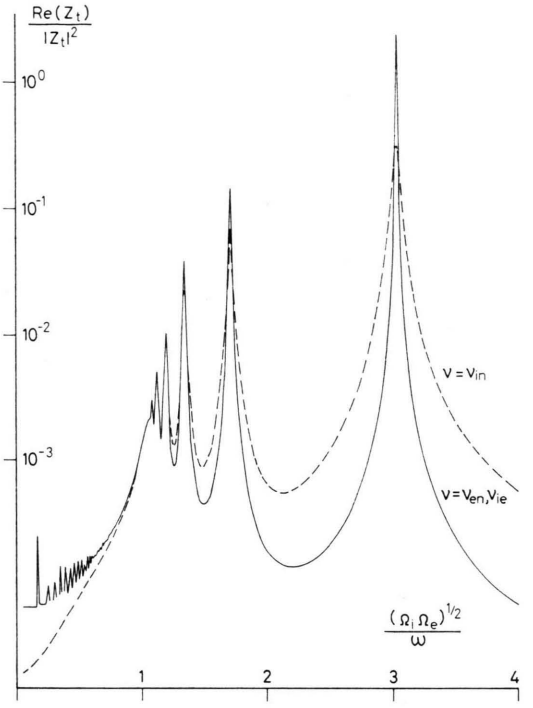

Fig. 11. Effective collision frequency studies for plasma with parameters of Figure 4. The effective collision frequency is $\nu = 4.7 \cdot 10^6\ \mathrm{s}^{-1}$.

described above still prevails for virtually all conditions of interest, in particular for those of Figures 7 and 8.

The varying influence of the three collision frequencies has to be taken into account when the lower hybrid frequency is not approximated by the geometrical mean cyclotron frequency, i. e. when the relation $\omega_{pe}^2 \gg \Omega_e^2$ is violated. However, similar conclusion as in previous cases can be drawn as far as the basic features of the power transfer are concerned.

V. Summary

In the absence of domineering coupling resonances of radial modes in the range $\omega < \omega_{LH}(k_{cr} \cdot p < \pi)$ electron and ion pressure may decisively influence the power transfer. This is likely to occur for plasmas of relatively low electron density and/or small radial extent. Moreover small values of $(\nu/\omega)^2/(p_e/B_0^2/2\mu_0)$ favour deviations from the predictions of the cold plasma treatment.

Acknowledgements

The support of these investigations by Landesamt für Forschung des Landes Nordrhein-Westfalen is gratefully acknowledged. These investigations are part of the joint efforts within the Sonderforschungsbereich „Plasmaphysik Bochum/Jülich".

Appendices

I. Modification of the Factors Occuring in the Dispersion Relation (5) of I.

$$\omega_i = \omega\left[1 + \frac{i}{\omega}\left\{\nu_{ie}\frac{\varrho_e}{\varrho_i+\varrho_e} + \nu_{in}\frac{\varrho_n}{\varrho_i+\varrho_n}\right\}\right], \tag{A 1}$$

$$\omega_e = \omega\left[1 + \frac{i}{\omega}\left\{\nu_{ie}\frac{\varrho_i}{\varrho_i+\varrho_e} + \nu_{en}\frac{\varrho_n}{\varrho_e+\varrho_n}\right\}\right], \tag{A 2}$$

$$\beta_i = \frac{\Omega_i}{\omega_i}\left[1 + \frac{\Omega_e}{\Omega_i}\frac{\nu_{ie}^2[\varrho_i\,\varrho_e/(\varrho_i+\varrho_e)^2]}{\omega_e^2-\Omega_e^2} - i\frac{\omega_e\,\Omega_i-\omega_i\,\Omega_e}{\Omega_i(\omega_e^2-\Omega_e^2)}\nu_{ie}\frac{\varrho_i}{\varrho_i+\varrho_e}\right]$$
$$\times\left[1 + \frac{\omega_e}{\omega_i}\frac{\nu_{ie}^2[\varrho_i\,\varrho_e/(\varrho_i+\varrho_e)^2]}{\omega_e^2-\Omega_e^2} - i\frac{\nu_{ie}^2[\varrho_i\,\varrho_e/(\varrho_i+\varrho_e)^2]+\omega_e\,\omega_i-\Omega_e\,\Omega_i}{\omega_i(\omega_e^2-\Omega_e^2)}\nu_{ie}\frac{\varrho_i}{\varrho_i+\varrho_e}\right]^{-1}, \tag{A 3}$$

$$\beta_e = \frac{\Omega_e}{\omega_e}\left[1 + \frac{\Omega_i}{\Omega_e}\frac{\nu_{ie}^2[\varrho_i\,\varrho_e/(\varrho_i+\varrho_e)^2]}{\omega_i^2-\Omega_i^2} - i\frac{\omega_i\,\Omega_e-\omega_e\,\Omega_i}{\Omega_e(\omega_i^2-\Omega_i^2)}\nu_{ie}\frac{\varrho_e}{\varrho_i+\varrho_e}\right]$$
$$\times\left[1 + \frac{\omega_i}{\omega_e}\frac{\nu_{ie}^2[\varrho_i\,\varrho_e/(\varrho_i+\varrho_e)^2]}{\omega_i^2-\Omega_i^2} - i\frac{\nu_{ie}^2[\varrho_i\,\varrho_e/(\varrho_i+\varrho_e)^2]+\omega_e\,\omega_i-\Omega_e\,\Omega_i}{\omega_e(\omega_i^2-\Omega_i^2)}\nu_{ie}\frac{\varrho_e}{\varrho_i+\varrho_e}\right]^{-1}, \tag{A 4}$$

$$A_i = \frac{\omega_{pi}^2/\omega\,\omega_i}{1-\Omega_i^2/\omega_i^2}\left[1 + \frac{\omega_e}{\omega_i}\frac{\nu_{ie}^2[\varrho_i\,\varrho_e/(\varrho_i+\varrho_e)^2]}{\omega_e^2-\Omega_e^2} - i\frac{\nu_{ie}^2[\varrho_i\,\varrho_e/(\varrho_i+\varrho_e)^2]+\omega_e\,\omega_i-\Omega_e\,\Omega_i}{\omega_i(\omega_e^2-\Omega_e^2)}\nu_{ie}\frac{\varrho_i}{\varrho_i+\varrho_e}\right]$$
$$\times\left[1 + \frac{\nu_{ie}^2[\varrho_i\,\varrho_e/(\varrho_i+\varrho_e)^2]+2(\omega_e\,\omega_i-\Omega_e\,\Omega_i)}{(\omega_e^2-\Omega_e^2)(\omega_i^2-\Omega_i^2)}\nu_{ie}^2\frac{\varrho_i\,\varrho_e}{(\varrho_i+\varrho_e)^2}\right]^{-1}, \tag{A 5}$$

$$A_e = \frac{\omega_{pe}^2/\omega\,\omega_e}{1-\Omega_e^2/\omega_e^2}\left[1+\frac{\omega_i}{\omega_e}\frac{\nu_{ie}^2[\varrho_i\,\varrho_e/(\varrho_i+\varrho_e)^2]}{\omega_i^2-\Omega_i^2}-i\frac{\nu_{ie}^2[\varrho_i\,\varrho_e/(\varrho_i+\varrho_e)^2]+\omega_e\,\omega_i-\Omega_e\,\Omega_i}{\omega_e(\omega_i^2-\Omega_i^2)}\nu_{ie}\frac{\varrho_e}{\varrho_i+\varrho_e}\right]$$
$$\times\left[1+\frac{\nu_{ie}^2[\varrho_i\,\varrho_e/(\varrho_i+\varrho_e)^2]+2(\omega_e\,\omega_i-\Omega_i\,\Omega_e)}{(\omega_e^2-\Omega_e^2)(\omega_i^2-\Omega_i^2)}\nu_{ie}^2\frac{\varrho_i\,\varrho_e}{(\varrho_i+\varrho_e)^2}\right]^{-1}. \tag{A 6}$$

II. Explicit Definitions of the Quantities in the Impedance Relation (3)

$$\frac{B_n}{A_n}=\frac{I_{i1}\,I_{e3}-I_{i3}\,I_{e1}}{I_{i3}\,I_{e2}-I_{i2}\,I_{e3}}, \tag{A 7}$$

$$\frac{B_n'}{A_n}=\frac{I_{i2}\,I_{e1}-I_{i1}\,I_{e2}}{I_{i3}\,I_{e2}-I_{i2}\,I_{e3}}, \tag{A 8}$$

$$I_{at}=K_{pat}\,k_t\,p\,J_n'(k_t\,p)-K_{uat}\,n\,J_n(k_t\,p),\ \alpha=\theta,\mathrm{e},\mathrm{i},\qquad t=1,2,3, \tag{A 9}$$

$$I_1=J_n'(k_0\,s)\,H_n'(k_0\,p)-J_n'(k_0\,p)\,H_n'(k_0\,s), \tag{A 10}$$

$$I_2=J_n'(k_0\,s)\,H_n(k_0\,p)-J_n(k_0\,p)\,H_n'(k_0\,s) \tag{A 11}$$

with
$$R_c=(\pi\,k_0\,s\,m)^2\,l/\varepsilon_0\,\omega, \tag{A 12}$$

$$\begin{aligned}
K_{p\Theta t}&=\bar K_r+(K_{\Theta e}\,\alpha_{0e}+K_{\Theta i}\,\alpha_{0i})-k_t^2(K_{\Theta e}\,\alpha_{1e}+K_{\Theta i}\,\alpha_{1i})+k_t^4(K_{\Theta e}\,\alpha_{2e}+K_{\Theta i}\,\alpha_{2i}),\\
K_{u\Theta t}&=i\,\bar K_\Theta+(K_{re}\,\alpha_{0e}+K_{ri}\,\alpha_{0i})-k_t^2(K_{re}\,\alpha_{1e}+K_{ri}\,\alpha_{1i})+k_t^4(K_{re}\,\alpha_{2e}+K_{ri}\,\alpha_{2i}),\\
K_{pet}&=K_{\Theta e}+\{(K_{re}-\beta_e\,K_{\Theta e}+1/A_e)\,\alpha_{0e}+K_{cr}\,\alpha_{0i}\}-k_t^2\{(K_{re}-\beta_e\,K_{\Theta e}+1/A_e)\,\alpha_{1e}+K_{cr}\,\alpha_{1i}\}\\
&\quad+k_t^4\{(K_{re}-\beta_e\,K_{\Theta e}+1/A_e)\,\alpha_{2e}+K_{cr}\,\alpha_{2i}\},\\
K_{uet}&=K_{re}+\{(K_{\Theta e}-\beta_e\,K_{re}-\beta_e/A_e)\,\alpha_{0e}+K_{c\Theta}\,\alpha_{0i}\}-k_t^2\{(K_{\Theta e}-\beta_e\,K_{re}-\beta_e/A_e)\,\alpha_{1e}+K_{c\Theta}\,\alpha_{1i}\}\\
&\quad+k_t^4\{(K_{\Theta e}-\beta_e\,K_{re}-\beta_e/A_e)\,\alpha_{2e}+K_{c\Theta}\,\alpha_{2i}\},\\
K_{pit}&=K_{\Theta i}+\{(K_{ri}+\beta_i\,K_{\Theta i}+1/A_i)\,\alpha_{0i}+K_{cr}\,\alpha_{0e}\}-k_t^2\{(K_{ri}+\beta_i\,K_{\Theta i}+1/A_i)\,\alpha_{1i}+K_{cr}\,\alpha_{1e}\}\\
&\quad+k_t^4\{(K_{ri}+\beta_i\,K_{\Theta i}+1/A_i)\,\alpha_{2i}+K_{cr}\,\alpha_{2e}\},\\
K_{uit}&=K_{ri}+\{(K_{\Theta i}+\beta_i\,K_{ri}+\beta_i/A_i)\,\alpha_{0i}+K_{c\Theta}\,\alpha_{0e}\}-k_t^2\{(K_{\Theta i}+\beta_i\,K_{ri}+\beta_i/A_i)\,\alpha_{1i}+K_{c\Theta}\,\alpha_{1e}\}\\
&\quad+k_t^4\{(K_{\Theta i}+\beta_i\,K_{ri}+\beta_i/A_i)\,\alpha_{2i}+K_{c\Theta}\,\alpha_{2e}\},
\end{aligned} \tag{A 13}$$

$$\begin{aligned}
\alpha_{0e}&=\frac{A_e\,\lambda_e^2}{\lambda_s^2}\left\{\frac{\beta_i}{A_e\,A_i}\,b_1+\beta_e\,k_0^2\,\lambda_i^2\,K_{cr}(K_r^2+K_\Theta^2)\right\},\\
\alpha_{1e}&=\frac{A_e\,\lambda_e^2}{\lambda_s^2}\left\{\frac{\beta_i}{A_i}\,\lambda_e^2(1-A_i)+\beta_e\,\lambda_i^2+\beta_i\,k_0^2\,\lambda_e^2\,\lambda_i^2\,[\beta_e\,\beta_i+K_{cr}(K_r^2+K_\Theta^2)]\right\},\\
\alpha_{2e}&=(A_e\,\lambda_e^2/\lambda_s^2)\,(\lambda_e^2\,\lambda_i^2\,\beta_i),\\
\alpha_{0i}&=\frac{A_i\,\lambda_i^2}{\lambda_s^2}\left\{\frac{\beta_e}{A_e\,A_i}\,b_2+\beta_i\,k_0^2\,\lambda_e^2\,K_{cr}(K_r^2+K_\Theta^2)\right\},\\
\alpha_{1i}&=\frac{A_i\,\lambda_i^2}{\lambda_s^2}\left\{\frac{\beta_e}{A_e}\,\lambda_i^2(1-A_e)+\beta_i\,\lambda_e^2+\beta_e\,k_0^2\,\lambda_i^2\,\lambda_e^2\,[\beta_e\,\beta_i+K_{cr}(K_r^2+K_\Theta^2)]\right\},\\
\alpha_{2i}&=(A_i\,\lambda_i^2/\lambda_s^2)\,(\lambda_e^2\,\lambda_i^2\,\beta_e),
\end{aligned} \tag{A 14}$$

$$\lambda_s^2=\lambda_e^2\,\beta_i(\beta_e+\beta_i-\beta_e/A_i)-\lambda_i^2\,\beta_e\,(\beta_e+\beta_i-\beta_i/A_e), \tag{A 15}$$

$$K_{cr}(K_r^2+K_\Theta^2)=1-A_e-A_i+\beta_i^2\,A_i+\beta_e^2\,A_e-\beta_e\,\beta_i, \tag{A 16}$$

$$K_{c\Theta}(K_r^2+K_\Theta^2)=\beta_i(1-A_e)-\beta_e(1-A_i)-\beta_e\,\beta_i(\beta_i\,A_i-\beta_e\,A_e), \tag{A 17}$$

$$b_1=k_0^2\,\lambda_e^2\,[(1-A_i)(1-A_e-A_i+\beta_e^2\,A_e)-\beta_i^2\,A_i^2], \tag{A 18}$$

$$b_2=k_0^2\,\lambda_i^2\,[(1-A_e)(1-A_e-A_i+\beta_i^2\,A_i)-\beta_e^2\,A_e^2], \tag{A 19}$$

$$\begin{aligned}
K_{rj}&=\bar K_r+\varepsilon_j\,\beta_j\,i\,\bar K_\Theta, & K_{\Theta j}&=i\,\bar K_\Theta+\varepsilon_j\,\beta_j\,\bar K_r, & j&=\mathrm{e},\mathrm{i},\\
\bar K_r&=K_r/(K_r^2+K_\Theta^2), & \bar K_\Theta&=K_\Theta/(K_r^2+K_\Theta^2),
\end{aligned} \tag{A 20}$$

$$K_r=1-A_e-A_i,\qquad i\,K_\Theta=(\beta_i\,A_i-\beta_e\,A_e),$$

$$\lambda_j^2=\frac{U_j^2/\omega\,\omega_j}{1-\Omega_j^2/\omega_j^2},\qquad U_j^2=\gamma_j\,K\,T_j/m_j. \tag{A 21}$$

It can immediately be ascertained that $T_i = 0$ amounts to $B_n' = 0$ in (1) and the suffix t has only the values 1 and 2. In that case (3) is identical to (39) of I; of course, the new definitions (A 1) – (A 6) have to be used in case of $\nu_{ie} \neq 0$. The expressions above – though formally retaining dependencies $e^{in\Theta}$ – are mainly derived for the case of the rotationally symmetric wave excitation with $n = 0$.

[1] R. BABU and H. SCHLÜTER, Z. Naturforsch. **26 a**, 856 [1971]. In the following this article is referred to as I.
[2] D. E. HASTI, M. E. OAKES, and H. SCHLÜTER, Plasma Phys. **12**, 1886 [1970].
[3] P. E. VANDENPLAS, A. M. MESSIAEN, J.-L. MONFORT, and J. J. PAPIER, Plasma Phys. **12**, 391 [1970].
[4] A. SCHLÜTER, Z. Naturforsch. **5 a**, 721 [1950]; **6 a**, 73 [1951].
[5] C. R. SKIPPING, M. E. OAKES, and H. SCHLÜTER, Phys. Fluids **12**, 1887 [1969].
[6] V. D. DEMIDOV, D. A. FRANK-KAMENTSKII, and V. L. YAKIMENKO, Sov. Physics – Tech. Phys. **7**, 875 [1963].
[7] M. E. OAKES and H. SCHLÜTER, Ann. Physics (N.Y.) **35**, 396 [1965].

Kinetische Prozesse in einem photochemischen Jodlaser *

K. HOHLA und K. L. KOMPA

Max-Planck-Institut für Plasmaphysik, Garching bei München
und Institut für Anorganische Chemie der Universität München

(Z. Naturforsch. **27 a**, 938—947 [1972]; eingegangen am 13. März 1972)

Kinetic Processes in a Photochemical Iodine Laser

Time-dependent gain measurements of a pulsed iodine laser amplifier have been used to determine decay rates of excited iodine atoms $5^2P_{1/2}$. Rate constants are reported for the iodine deactivation by CF_3I and C_2F_6. Attempts to correlate the results with predictions from a kinetic model indicate that excited iodine atoms are formed not only in the primary photolysis but also by additional chemical processes.

Das Potential chemischer Laser für reaktionskinetische Untersuchungen ist mehrfach hervorgehoben worden [1–4], doch sind die experimentellen Belege bislang noch spärlich. In der Mehrzahl der chemischen Laserarbeiten mit reaktionskinetischer Zielsetzung wird die Interpretation von Emissionssignalen aus chemischen Laseroszillatoren angestrebt. Das ist insofern eine schwierige Aufgabe als eine umfassende Behandlung von Resonatorparametern, Modenstruktur und Anschwingverhalten erforderlich ist. Bei der „equal-ain"-Methode von PARKER und PIMENTEL [5] können diese Schwierigkeiten teilweise vermieden werden, es müssen jedoch andererseits zusätzliche Ungenauigkeiten in Kauf genommen werden [6].

Wir haben in der vorliegenden Arbeit den Versuch unternommen, den Bereich der Oszillatormessungen zu verlassen und aus zeitabhängigen Verstärkungsmessungen kinetische Informationen zu gewinnen [7]. Dabei wird zu verschiedenen Zeiten nach dem Photolyselichtblitz mit Hilfe eines kurzen Oszillatorpulses (Pulsdauer ~ 100 nsec) die Besetzungsinversion und damit die Konzentration an angeregten Teilchen gemessen. Solange Kleinsignalverstärkungsmessungen betrachtet werden (s. u.), unterscheidet sich das Verfahren, das auch als kinetische Verstärkungsspektroskopie bezeichnet wird, im Prinzip nicht von der Methode zeitabhängiger Absorptionsmessungen, die etwa der kinetischen Blitzspektroskopie zugrunde liegt. Es ist überall da anwendbar, wo geeignete Laser-Meßlichtquellen zur Verfügung stehen.

In der Photodissoziation von Alkyljodiden RJ (R = Alkyl oder Fluoralkyl) entstehen elektronisch angeregte Jodatome im Zustand $5^2P_{1/2}$, so daß nach der Blitzphotolyse eine Überbesetzung gegenüber dem Grundzustand $5^2P_{3/2}$ vorliegt. Diese Besetzungsinversion führt für kurze Zeit zum Auftreten von

Sonderdruckanforderungen an Dr. K. L. KOMPA, Max-Planck-Institut für Plasmaphysik, *D-8046 Garching* bei München.

* Die dieser Arbeit zugrunde liegenden Untersuchungen wurden mit Mitteln des Bundesministeriums für Bildung und Wissenschaft im Rahmen des Technologieprogrammes gefördert.